

Outward Currents Influencing Bursting Dynamics in Guinea Pig Trigeminal Motoneurons

CHRISTOPHER A. DEL NEGRO, CHIE-FANG HSIAO, AND SCOTT H. CHANDLER

Department of Physiological Science, University of California, Los Angeles, California 90095-1568

Del Negro, Christopher A., Chie-Fang Hsiao, and Scott H. Chandler. Outward currents influencing bursting dynamics in guinea pig trigeminal motoneurons. *J. Neurophysiol.* 81: 1478–1485, 1999. To initiate and maintain bursts (and plateau potentials) in the presence of serotonin, guinea pig trigeminal motoneurons utilize L-type Ca^{2+} and persistent Na^+ inward currents. However, the intrinsic currents that contribute to burst termination and determine the duration of the interburst interval are unknown. Therefore we investigated the roles of outward currents, whose slow activation is coupled to cytosolic cation (Ca^{2+} and Na^+) accumulation. First we examined a Ca^{2+} -dependent K^+ current ($I_{\text{K-Ca}}$) with apamin and Ba^{2+} -substituted, low- Ca^{2+} solution. Blockade of $I_{\text{K-Ca}}$ lengthened burst duration and cycle time but did not abolish bursting. Next we studied the Na^+/K^+ -ATPase pump current (I_p) with cardiac glycosides. In the presence of apamin or low- $\text{Ca}^{2+}/\text{Ba}^{2+}$ solution, blocking I_p (with ouabain or strophanthidin) decreased both burst duration and cycle time and ultimately transformed bursting into tonic spiking. We conclude that $I_{\text{K-Ca}}$ and I_p contribute to burst termination in trigeminal motoneurons. These currents influence temporal bursting properties such as burst duration and cycle time and may help determine the phasic activity of motoneurons during rhythmic oral-motor behaviors.

cumulation (Gorman et al. 1981, 1982; Li and Hatton 1996; Rose and Ransom 1997). For example, inward Ca^{2+} current can activate Ca^{2+} -dependent K^+ currents during bursts (Legendre et al. 1985; Tell and Jean 1993) or cause Ca^{2+} -dependent Ca^{2+} current inactivation (Benson and Adams 1989; Canavier et al. 1991; Heyer and Lux 1976; Kramer and Zucker 1985). Na^+ currents can activate the Na^+/K^+ -ATPase pump during bursts (Johnson et al. 1992; Li et al. 1996; Tsai and Chen 1995) or possibly experience voltage- or cytosolic Na^+ -dependent inactivation (Fleidervish et al. 1996).

In trigeminal motoneurons that innervate jaw musculature both Ca^{2+} and Na^+ currents are important for serotonin-induced bursting (Hsiao et al. 1998). Therefore intracellular accumulation of Ca^{2+} and Na^+ ions may activate distinct slow repolarizing currents. Here we test the hypothesis that an apamin-sensitive, Ca^{2+} -dependent K^+ current ($I_{\text{K-Ca}}$) and a cardiac glycoside-sensitive Na^+/K^+ -ATPase pump current (I_p) activated by intracellular Ca^{2+} and Na^+ , respectively, contribute to burst termination and the overall dynamics of bursting behavior.

INTRODUCTION

Neuronal bursting behavior, by a traditional mechanism (Del Negro et al. 1998), utilizes non- or slowly inactivating inward currents to generate a region of negative slope resistance in the steady-state current-voltage (I - V) relationship. This region of negative slope resistance creates two stable membrane states on either side of spike threshold: one quiescent state and another suprathreshold or active state, at which the cell discharges tonically. These two states are traversed during the quiescent and active phases of bursting.

To initiate individual bursts, the inward currents underlying the negative slope resistance cause rapid depolarization, which shifts the membrane potential from its quiescent to active state (see Fig. 3B of Del Negro et al. 1998). Conversely, bursts terminate because of much slower membrane processes that generate repolarizing currents (Bertram et al. 1995; Rinzel and Ermentrout 1998). During the active phase these steadily growing currents cause a decline in intraburst spike frequency and ultimately a return to quiescence. The source of the repolarizing currents can be a distinct set of ion channels, intramembranous ion pumps, the slow inactivation of inward currents, or a combination of these factors. The repolarizing currents that terminate bursts are usually activated by cytosolic cation ac-

METHODS

Trigeminal motoneurons were recorded intracellularly in 450- μm -thick transverse brain stem slices from adolescent guinea pigs (150–250 g), as shown previously (Chandler et al. 1994; Hsiao et al. 1998). Slices were perfused in a gas-interface chamber at 34°C with oxygenated Ringer solution containing (in mM) 130.0 NaCl, 3.0 KCl, 1.25 KH_2PO_4 , 20.0 NaHCO_3 , 10.0 D-glucose, 2.4 CaCl_2 , and 1.3 MgSO_4 . Microelectrodes were filled with 3 M KCl (15–20 M Ω). Current-clamp experiments were performed with an Axoclamp 2A amplifier in bridge mode (Axon Instruments, Burlingame, CA).

The acceptance criteria for trigeminal motoneurons included resting potential less than -50 mV, input resistance of 6–18 M Ω , and action potential amplitude >60 mV (Chandler et al. 1994; Curtis and Apenteng 1993).

Bath-applied drugs were effective after ~ 3.5 min of perfusion; complete solution change required ~ 20 min. We used 10 μM serotonin (Sigma Chemical, St. Louis, MO) to elicit bursting; this dose reliably induces bistability and bursting in trigeminal motoneurons (Hsiao et al. 1998). Other drugs were used at the following concentrations: apamin (0.2 μM , Sigma), ouabain (6 μM , Sigma), and strophanthidin (4 μM , Sigma). In some experiments Ca^{2+} concentration was lowered to 0.4 mM and substituted with Ba^{2+} on an equimolar basis.

Bursting characteristics such as the time of burst onset and termination and intraburst spike frequency were measured with Datapac III v0.1.47 (Run Technologies, Irvine, CA). Burst duration was defined as the mean time from burst onset to termination in three or more consecutive bursts. Burst cycle time was defined as the mean time from burst onset to onset in three or more consecutive cycles. Means

The costs of publication of this article were defrayed in part by the payment of page charges. The article must therefore be hereby marked "advertisement" in accordance with 18 U.S.C. Section 1734 solely to indicate this fact.

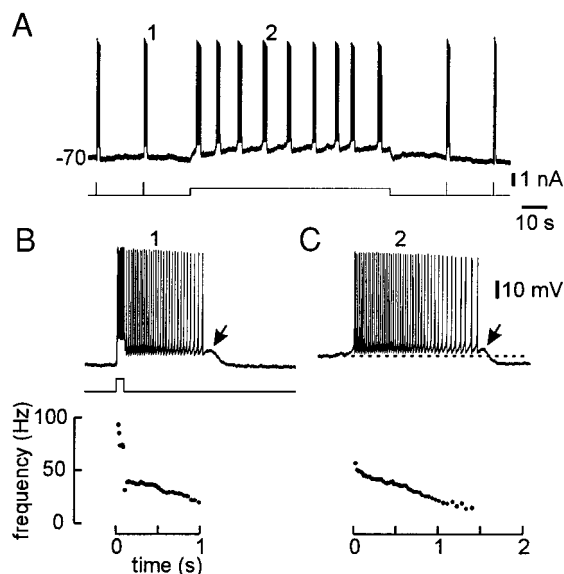


FIG. 1. Serotonin-induced plateau potentials and bursting in trigeminal motoneurons. *A*: from resting potential (-70 mV), plateau potentials could be evoked by 300-ms, 1-nA current pulses (*bottom trace*). Continuous bursting activity was evoked by adding a constant current bias of 0.5 nA. By removing the depolarizing current bias, the cell reestablished its resting membrane potential and again exhibited plateau potentials in response to the transient stimuli. The current calibration applies to *A* and *B*. The time calibration applies only to *A*. *B* and *C*: plateau potential (*B*) and a burst (*C*) from the record in *A* (responses labeled 1 and 2, respectively) are displayed with an expanded time scale. For each response, the instantaneous intraburst spike frequency is plotted synchronously below the voltage trajectory. The voltage calibration in *C* applies to all traces. Time calibrations for *B* and *C* are displayed as the abscissa of the frequency-time (f - t) plot (*bottom*).

are reported as \pm SE. Pharmacologically induced changes in bursting characteristics were tested for each cell individually with unpaired Student's t -tests (SYSTAT 7.0, SPSS, Chicago, IL).

RESULTS

In the presence of serotonin, trigeminal motoneurons exhibit plateau potentials and spontaneous rhythmic bursting (Hsiao et al. 1998). Figure 1 illustrates these behaviors in a typical cell. At resting potential, the cell was bistable. Therefore transient stimuli evoked plateau potentials (Fig. 1, *A* and *B*, $n = 135$, including cells from our earlier paper) (Hsiao et al. 1998). This behavior could be converted to continuous bursting activity by injecting depolarizing constant current (Fig. 1, *A* and *C*, $n = 90$). In all cells recorded, burst duration ranged from 0.7 to 53 s, the interburst interval ranged from 4.2 to 123 s, and the cycle time ranged from 4.9 to 178 s.

Several features of the plateau potentials and bursts suggest that repolarizing currents were recruited throughout the active phase. First, during the plateau potentials and bursts, spike frequency declined monotonically until burst termination (Fig. 1, *B* and *C*, *bottom*), which is characteristic of a traditional, negative slope resistance-based bursting mechanism (Bertram et al. 1995; Del Negro et al. 1998). Also a hump-like depolarizing afterpotential occurred at burst termination. This suggests that the voltage trajectory rose after the previous spike but failed to reach threshold putatively because of the growing repolarizing current (Fig. 1, *B* and *C*, arrows). Last, after burst termination, the membrane potential was hyperpolarized by 5 mV compared with burst onset, suggesting the growth of

outward currents during the burst (Fig. 1*C*, broken line inserted for reference).

Role of Ca^{2+} -dependent K^+ current

L-type Ca^{2+} currents provide the majority of inward current needed for serotonin-induced bursting (Hsiao et al. 1998). Because Ca^{2+} may accumulate intracellularly during bursts and trigeminal motoneurons express an apamin-sensitive, Ca^{2+} -dependent K^+ current (Chandler et al. 1994; Kobayashi et al. 1997), we tested whether I_{K-Ca} was involved in the burst termination. Specifically, we applied apamin ($n = 5$) or Ba^{2+} -substituted, low- Ca^{2+} solution ($n = 4$) to reduce or eliminate I_{K-Ca} .

Apamin typically prolonged burst duration and extended the cycle time. In Fig. 2*A* mean burst duration increased significantly from 47 ± 2 to 271 ± 30 s ($P < 0.001$), and mean cycle time increased from 115 ± 5 to 490 ± 46 s ($P < 0.001$) in the presence of apamin. In general, apamin significantly increased burst duration by $313 \pm 76\%$ ($n = 5/5$, $P < 0.01$) and extended burst cycle time by $202 \pm 58\%$ ($n = 4/5$, $P < 0.05$). In addition to increasing burst duration and cycle time, apamin

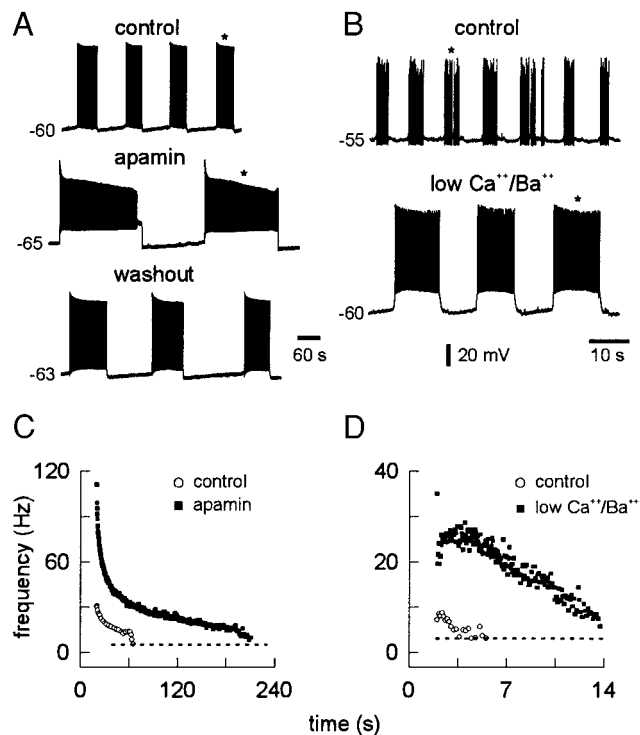


FIG. 2. Role of a Ca^{2+} -dependent K^+ current (I_{K-Ca}) in burst termination. *A*: during serotonin-induced bursting, apamin reversibly lengthened burst duration and cycle time. Time calibration is shown; 0.2 nA of bias current was applied during washout. *B*: during serotonin-induced bursting in a different motoneuron, Ba^{2+} -substituted, low- Ca^{2+} solution (low Ca^{2+}/Ba^{2+}) caused similar enhancement of burst duration and cycle time. Time calibration is shown. The voltage calibration in *B* applies to *A* and *B*. Holding currents in control and low- Ca^{2+}/Ba^{2+} conditions were -0.3 and -0.5 nA, respectively. *C*: instantaneous intraburst spike frequency is plotted vs. time (f - t) plot for control (\circ) and apamin (\blacksquare) conditions. A broken horizontal line was inserted for reference at the level of 5 Hz because this was the spike frequency near which bursts terminated. *D*: similar f - t plots comparing control (\circ) and low- Ca^{2+}/Ba^{2+} (\blacksquare) conditions. A broken horizontal reference line was inserted at 3 Hz. Individual bursts represented in the f - t plots are marked in *A* and *B* with *.

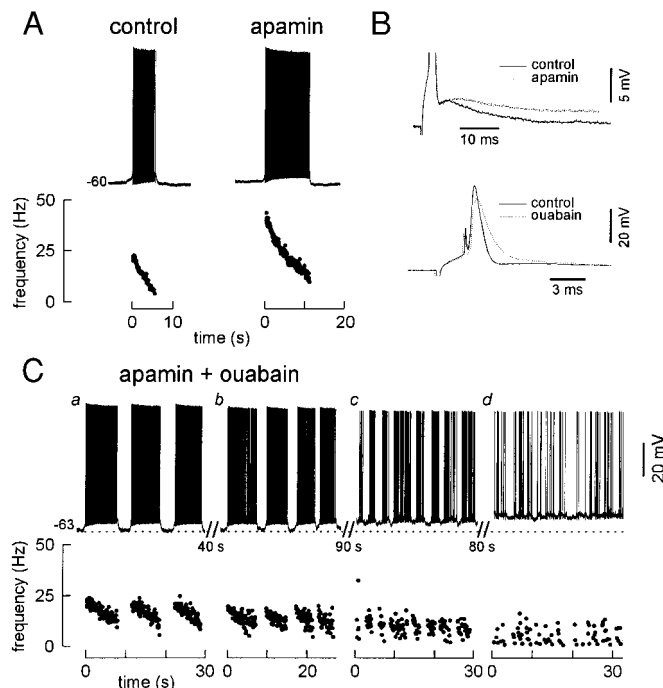


FIG. 3. Effects of apamin and apamin + ouabain on bursting characteristics. All data were obtained from the same cell. *A*: individual bursts in control (left) and apamin (right) conditions during serotonin-induced bursting. Intraburst spike frequency is plotted synchronously below the voltage traces. Time calibration plotted as the abscissa of the f - t plots. *B*: effects of apamin (top traces) and apamin + ouabain (bottom traces) on the action potential elicited by 3-ms rheobasic current stimuli. Superimposed top traces illustrate the blockade of the medium-duration afterhyperpolarization by apamin (---); spikes were truncated. Voltage and time calibrations apply to top traces only. Superimposed bottom traces show the ~20% decline in action potential amplitude caused by ouabain (---). The action potential under apamin + ouabain conditions was measured during the tonic spiking state shown in *Cd*. Holding current was -0.4 nA. Voltage and time calibrations apply to bottom traces only. *C*: serotonin-induced bursting, continued from *A*. Ouabain was bath applied 2 min before the start of this record. Instantaneous intraburst spike frequency is plotted synchronously below the voltage trajectory, time calibration shown in the abscissa of the f - t plots, and time breaks in the recording are indicated. Holding current was -0.5 nA. The voltage calibration in *C* applies to *A* and *C*.

also elevated the intraburst spike frequency-time (f - t) relationship (Fig. 2C), consistent with its suppression of the medium-duration afterhyperpolarization (mAHP) in trigeminal motoneurons (Fig. 3B) (Chandler et al. 1994; Hsiao et al. 1997; Kobayashi et al. 1997).

We also tested the role of I_{K-Ca} with Ba^{2+} -substituted, low- Ca^{2+} solution because Ba^{2+} can penetrate Ca^{2+} channels but does not activate I_{K-Ca} . Similar to apamin, low- Ca^{2+}/Ba^{2+} solution enhanced burst duration and cycle time. In Fig. 2B mean burst duration increased significantly from 3.5 ± 0.2 to 11.9 ± 0.6 s ($P < 0.001$), and mean cycle time increased from 9.0 ± 0.5 to 22.0 ± 0.8 s ($P < 0.001$). In general, low Ca^{2+}/Ba^{2+} significantly increased burst duration by $357 \pm 142\%$ ($n = 3/4$, $P < 0.01$) and extended cycle time by $271 \pm 76\%$ ($n = 3/4$, $P < 0.001$). Like apamin, low- Ca^{2+}/Ba^{2+} solution also elevated the intraburst f - t curve (Fig. 2D). The elevation in spike frequency could be caused by suppression of the mAHP, blockade of Ba^{2+} -sensitive K^+ channels (Hsiao et al. 1997), or a combination of both effects.

Although apamin and low- Ca^{2+}/Ba^{2+} solution upwardly shifted the intraburst f - t relationship, bursts still terminated (in

the absence of I_{K-Ca}) when the instantaneous intraburst spike frequency declined to low values similar to control. In Fig. 2C, spike frequency at the time of burst termination was 5 Hz in control and 8 Hz in the presence of apamin. In Fig. 2D, the spike frequency was 3 Hz in control and 5 Hz in low- Ca^{2+}/Ba^{2+} solution. These data suggest that the net outward current at the time of burst termination was similar in the presence or absence of I_{K-Ca} . Therefore some compensatory mechanism(s) must be present to terminate bursts after the blockade of I_{K-Ca} .

Role of Na^+/K^+ -ATPase pump

If I_{K-Ca} was the only outward current controlling spike frequency decline and burst termination, we would expect apamin or low- Ca^{2+}/Ba^{2+} solution to induce tonic spiking (because bursts would not be able to terminate). However, bursting continued in apamin or low- Ca^{2+}/Ba^{2+} conditions, suggesting additional sources of slow repolarizing current. Because transient and persistent Na^+ currents contribute to serotonin-induced bursting in trigeminal motoneurons (Hsiao et al. 1998), cytosolic Na^+ accumulation might also activate slow repolarizing current, analogous to Ca^{2+} , or cause slow Na^+ current inactivation. The Na^+/K^+ -ATPase pump is associated with bursting behavior (Johnson et al. 1992; Li et al. 1996; Tsai and Chen 1995), is activated by cytosolic Na^+ , and is electrogenic (because of pump stoichiometry: 3 Na^+ ions extruded for every 2 K^+ ions that enter) (Läuger 1991). Therefore we tested the potential contribution of the Na^+/K^+ -ATPase pump current (I_p) with cardiac glycosides ouabain ($n = 8$) and strophanthidin ($n = 6$), which block pump activity.

To determine the role of I_p we first applied apamin ($n = 4$, Fig. 3A) or low- Ca^{2+}/Ba^{2+} solution ($n = 4$, Fig. 4A) to block I_{K-Ca} . Once apamin or low Ca^{2+}/Ba^{2+} was effective, as measured by blockade of the mAHP (Fig. 3B, top), ouabain was added to block I_p . In all trigeminal motoneurons tested, ouabain ultimately abolished bursting and induced tonic spiking. Nevertheless, in three of four cells exposed to apamin + ouabain (Fig. 3C) and two of four cells exposed to low Ca^{2+}/Ba^{2+} + ouabain (Fig. 4A), bursting activity continued during a transition period that preceded tonic spiking.

During this transitional bursting phase, ouabain decreased burst duration and cycle time and reduced the amplitude of the postburst afterhyperpolarization (AHP). In Fig. 3, burst duration decreased significantly from 10.1 ± 1.0 to 7.6 ± 0.4 s ($P < 0.05$), and cycle time decreased from 29.8 ± 5.2 to 10.6 ± 0.3 s ($P < 0.001$) (measured at the temporal midpoint between the time of ouabain application and the time at which motoneurons assumed tonic spiking). Also ouabain reduced the postburst AHP, as measured during the interburst interval (Fig. 3C, broken line inserted for reference). In low- Ca^{2+}/Ba^{2+} solution, ouabain similarly decreased burst duration and cycle time and reduced the postburst AHP (Fig. 4A). In general, ouabain significantly decreased burst duration to $54 \pm 11\%$ of burst duration in the presence of apamin alone ($n = 3/3$, $P < 0.05$) and to 68% of burst duration in low- Ca^{2+}/Ba^{2+} solution ($n = 1/2$, $P < 0.05$). Moreover, ouabain decreased cycle time to $6 \pm 2\%$ of cycle time in the presence of apamin alone ($n = 3/3$, $P < 0.001$) and to 33% of cycle time in low- Ca^{2+}/Ba^{2+} solution ($n = 2/2$, $P < 0.001$).

Ouabain ultimately eliminated bursting. When I_{K-Ca} alone was blocked the intraburst f - t curve shifted upward but re-

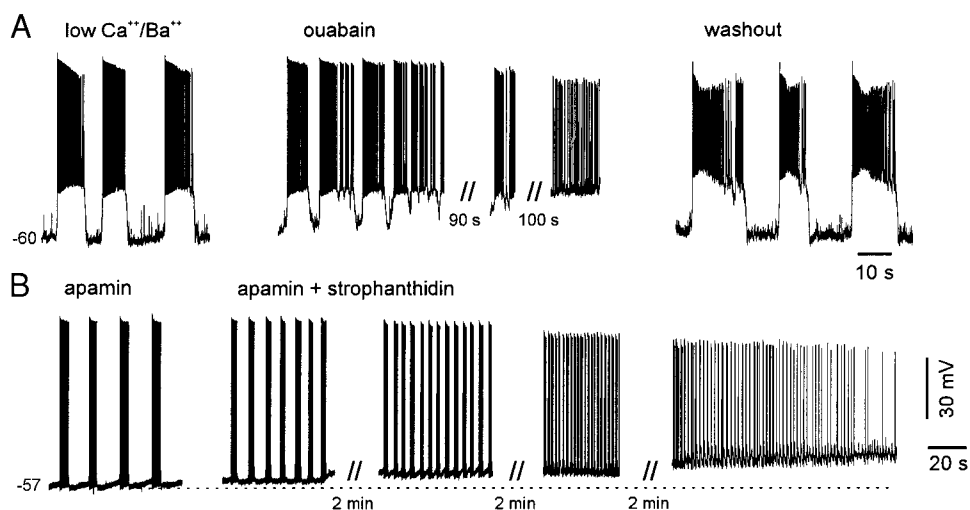


FIG. 4. Effects of ouabain and strophanthidin on bursting characteristics. *A*: serotonin-induced bursting in low-Ca²⁺/Ba²⁺ solution before (*left*), during (*middle*), and after (*right*) recovery from ouabain application. A bias current of -0.7 nA was applied during control and ouabain conditions; -0.6 nA was applied during washout. Time calibration applies only to *A*; time breaks in the recording during ouabain application are shown. *B*: serotonin-induced bursting in the presence of apamin (*left*) and apamin + strophanthidin (*right*) conditions; 0.1 nA holding current was applied during the entire experiment. Time calibration applies only to *B*. Voltage calibration applies to *A* and *B*.

remained smooth and monotonic (Figs. 2, *C* and *D*, and 3*A*). When ouabain was added burst duration, burst cycle time, and the postburst AHP all decreased. Later in the experiment ouabain disrupted the smooth monotonic decline in intraburst spike frequency, the hallmark of stable bursting activity. The intraburst *f-t* curve became erratic and then broke down completely (Fig. 3, *Cb-d*). Finally, the combined block of I_{K-Ca} and I_p prevented the rhythmic alternation of active and quiescent bursting phases. Instead, trigeminal motoneurons assumed the tonic spiking state shown in Figs. 3*Cd* and 4*A* (*middle panel*). This suggests that cells entered an active phase that could not terminate, putatively caused by blockade of both slow repolarizing currents, I_{K-Ca} and I_p .

During the nonterminating active phase, action potentials declined slightly in amplitude, $\sim 20\%$ (Fig. 3*B*, *bottom*), and repolarized more slowly, suggesting that ouabain affected the Na⁺ and K⁺ concentration gradients to some extent. In the remaining cells exposed to apamin + ouabain ($n = 1/4$) and low-Ca²⁺/Ba²⁺ + ouabain ($n = 2/4$) the transition to tonic spiking occurred rapidly, and a transient period of bursting activity was indecipherable (not shown).

To further test the role of I_p , we repeated these experiments with the cardiac glycoside strophanthidin. This drug was applied sequentially, after apamin, with the same criteria as the ouabain experiments ($n = 6$). Strophanthidin, like ouabain, ultimately abolished bursting and induced a nonterminating active phase (Fig. 4*B*). Three of six cells exposed to strophanthidin exhibited an analyzable transitional bursting phase. Similar to ouabain, strophanthidin decreased burst duration and cycle time. In Fig. 4*B*, burst duration decreased significantly from 4.4 ± 0.2 to 1.5 ± 0.2 s ($P < 0.01$), and cycle time decreased from 11.3 ± 0.8 to 2.9 ± 0.2 s ($P < 0.001$) (measured at the temporal midpoint between the time of strophanthidin application and the time at which cells assumed tonic spiking). Strophanthidin, similar to ouabain, reduced the postburst AHP (Fig. 4*B*, broken line inserted for reference). In general, strophanthidin significantly decreased burst duration to 54% of burst duration in the presence of apamin alone ($n = 2/3$, $P < 0.001$) and decreased cycle time to 43% of cycle time in apamin alone ($n = 3$, $P < 0.001$). One-half of the trigeminal motoneurons exposed to strophanthidin ($n = 3/6$) rapidly assumed tonic spiking without a discernable transitional bursting phase (not shown).

The nonterminating active phase induced by blockade of I_{K-Ca} and I_p could be manually terminated by extrinsic current injection ($n = 8$). Figure 5 shows a typical cell in the presence of apamin + strophanthidin. Under these conditions rapid burst termination only occurred after repolarizing current injection, whereas bursts initiated spontaneously 10–20 s after readjustment of current bias. These data suggest that the motoneurons still possessed a region of negative slope resistance in the steady-state *I-V* curve and could initiate bursts (the relationship between the negative slope resistance and burst initiation is explained by Del Negro et al. 1998) but did not possess sufficient intrinsic slow repolarizing processes to terminate bursts autonomously.

To investigate how I_p influences intraburst spike frequency and the membrane potential trajectory after burst termination, we performed the following experiment. In the absence of serotonin, we applied apamin to trigeminal motoneurons and simulated bursts by applying current pulses of variable magnitude (2–4 nA) and duration (0.4–13.6 s). For each simulated burst, we examined 1) the postburst AHP after termination of the stimulus pulse and 2) the intraburst *f-t* relationship. We then compared these measures in control versus ouabain ($n = 6$) or strophanthidin ($n = 1$) conditions. In all cells tested ouabain blocked the postburst AHP (Fig. 6*A*, *inset*), suggesting that I_p activated during the simulated burst and produced the ouabain-sensitive AHP at burst termination. Ouabain also shifted the intraburst *f-t* relationship upward, which further

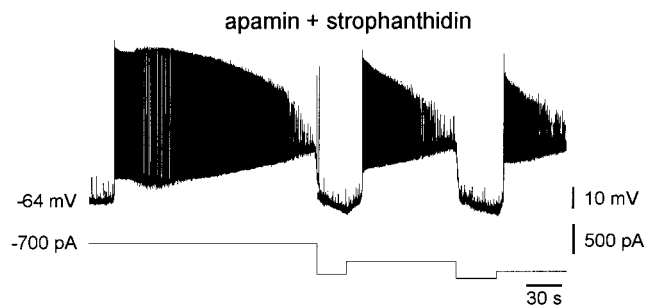


FIG. 5. Effects of extrinsic current on nonterminating bursts in the presence of apamin + strophanthidin (and serotonin). Hyperpolarizing current injection caused rapid burst termination. After burst termination, readjustment of the bias current allowed subsequent bursts to initiate autonomously after 10–20 s. All voltage, current, and time calibrations are shown.

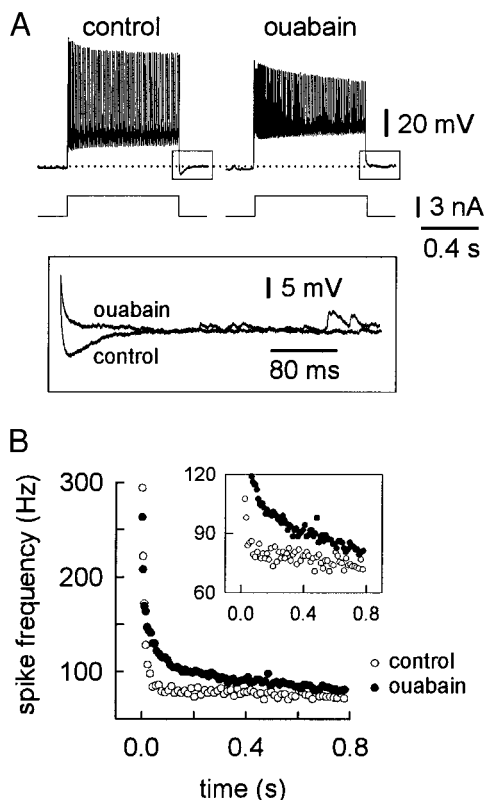


FIG. 6. Effects of ouabain on simulated bursts. *A*: membrane voltage responses to 3 nA, 0.8 s current pulses in the presence of apamin, before (*left*) and after (*right*) application of ouabain; -0.4 nA of bias current of was applied in ouabain conditions to maintain membrane potential at -65 mV. Voltage, current, and time calibrations are shown. *Inset*: postburst afterhyperpolarization for control and ouabain conditions (superimposed from *top traces*) in an expanded scale; separate voltage and time calibrations are shown. *B*: f - t plots comparing intraburst spike frequency in control (\circ) and ouabain (\bullet) conditions. *Inset*: same data on an expanded ordinate axis. Serotonin was not employed for this experiment.

suggests that I_p normally activated during the simulated burst and constrained intraburst spike frequency (Fig. 6*B*).

DISCUSSION

We examined slow outward currents activated by cytosolic cation accumulation that terminate serotonin-induced bursts in trigeminal motoneurons. We found that I_{K-Ca} and I_p both substantially contribute to burst termination and influence temporal bursting characteristics such as burst duration and the interburst interval. Therefore I_{K-Ca} and I_p probably influence the motoneuronal burst-like patterns that occur during rhythmic oral-motor behaviors (Goldberg and Chandler 1990; Goldberg et al. 1982; Gurahian et al. 1989).

During bursting by a traditional mechanism (Del Negro et al. 1998) neurons phasically alternate between quiescent and active membrane states. Stable membrane states are formed whenever the sum of intrinsic inward and outward currents equals zero and slope conductance is positive. This occurs where the steady-state I - V relationship intersects its zero-current axis with positive slope. If such an intersection occurs at a voltage less than spike threshold that state is quiescent; if it occurs at a voltage greater than threshold tonic spiking results. To simultaneously possess two stable states neurons must

express a region of negative slope resistance in their steady-state I - V relationship, which can twice intersect the zero-current axis with positive slope.

The inward currents underlying the region of negative slope resistance provide the structural framework for bistability (plateau potentials) and bursting by creating stable membrane states on either side of spike threshold, quiescent and tonic spiking, separated in the I - V relationship by the region of regenerative inward current. Therefore how do bistable or bursting cells move from state to state; what controls the dynamics?

To answer this, we address 1) how membrane potential first moves from its quiescent to active state, thereby initiating a plateau potential or burst, and 2) what slow repolarizing processes activate during the burst to diminish intraburst spike frequency and ultimately terminate the active phase.

Burst initiation

Trigeminal motoneurons utilize L-type Ca^{2+} and persistent Na^+ currents to initiate and maintain plateau potentials and bursts (Hsiao et al. 1998). Serotonin transforms membrane properties by inducing the necessary region of negative slope resistance and negatively shifting the I - V relationship so that the region of negative slope resistance often lies below the zero-current axis in the region of net inward current (Chandler and Trueblood 1995; Hsiao et al. 1998). In this case the only stable membrane state is the tonic spiking state, at a depolarized membrane potential. Therefore bursts initiate autonomously (Figs. 1*C* and 2 of Del Negro et al. 1998).

Sometimes the effects of serotonin are insufficient to shift the region of negative slope resistance fully into the region of net inward current. In this case, the I - V curve intersects the zero-current axis three times (twice with positive slope), and the cell is bistable. Then from the resting state plateau potentials can be initiated by transient stimuli (e.g., Fig. 1*B*). Adding depolarizing current bias can extrinsically shift the I - V relationship so that the negative slope region lies in the area of net inward current, transforming bistability into bursting, as shown in Fig. 1*A*.

Burst termination: the role of I_{K-Ca}

Of the slow repolarizing processes that terminate plateau potentials and bursts in trigeminal motoneurons, we first identified I_{K-Ca} . Because the blockade of I_{K-Ca} (by using apamin or low- Ca^{2+} / Ba^{2+} solution) lengthened burst duration and upwardly shifted the intraburst f - t curve, we propose that I_{K-Ca} normally activates during bursts caused by Ca^{2+} influx and accumulation, constrains intraburst spike frequency, and helps expedite burst termination. These effects are consistent with how I_{K-Ca} is recruited and affects spike frequency in a variety of mammalian motoneurons (Hounsgaard et al. 1988b; Mosfeldt Laursen and Rekling 1989; Nishimura et al. 1989; Takahashi 1990; Viana et al. 1993; Zhang and Krnjevic 1987), including trigeminal motoneurons (Chandler et al. 1994; Kobayashi et al. 1997). I_{K-Ca} similarly contributes to burst termination during conditional bursting in several other cell types (el Manira et al. 1994; Hu and Bourque 1992; Legendre et al. 1985; Tell and Jean 1993; Wallen and Grillner 1987), including *N*-methyl-D-aspartate (NMDA)-induced bursting in trigeminal motoneurons (Kim and Chandler 1995).

However, additional slow processes must influence burst termination in trigeminal motoneurons. When I_{K-Ca} was blocked bursting activity continued. In the absence of I_{K-Ca} spike frequency was 5–8 Hz at the time of burst termination, which was similar to the spike frequency at the time of burst termination in control (3–5 Hz, Fig. 2). This suggests that in all conditions the net outward current was comparable at the end of the active phase. Although I_{K-Ca} normally contributes to burst termination, additional repolarizing processes compensate for I_{K-Ca} loss under apamin or low- Ca^{2+}/Ba^{2+} conditions and generate sufficient repolarizing current to terminate the active phase. However, when I_{K-Ca} is reduced or eliminated the remaining slow processes require more time to generate the requisite outward current, consequently lengthening burst duration. The extended cycle time during blockade of I_{K-Ca} most likely reflects the slower time course of relaxation of these compensatory slow repolarizing processes.

Burst termination: the role of I_p

The other slow repolarizing process, which assists I_{K-Ca} to terminate plateau potentials and bursts, is constituted primarily by I_p because removal of I_p ultimately blocks serotonin-induced bursting. If slow inactivation of either the persistent Na^+ or the L-type Ca^{2+} channels contributed substantially to burst termination we would expect bursts to terminate even when I_{K-Ca} and I_p are both blocked. However, the combined block of I_{K-Ca} and I_p always transformed rhythmic bursting into a nonterminating active phase of tonic spiking (Figs. 3 and 4).

We propose that the role of I_p is multifaceted and that the pump current is composed of both steady-state and dynamic components. We base our conclusions on the effects of the cardiac glycosides during the transitional bursting phase that preceded tonic spiking in some cells. First, cardiac glycosides dramatically decreased burst cycle time. Neurons constantly extrude Na^+ via the Na^+/K^+ pump (Läuger 1991). Therefore the electrogenic nature of the pump normally creates a “background” outward current. This steady-state component of I_p will affect the voltage trajectory most effectively when membrane conductance is low, which corresponds to the interburst interval. In trigeminal motoneurons, blocking this maintained outward current (i.e., the steady-state component of I_p) with cardiac glycosides shortens cycle time by effectively increasing the contribution of the inward currents during the interburst interval and thereby hastens burst onset. Sakai et al. (1996) similarly argue that the steady-state component of I_p in rabbit sinoatrial node cells influences the pacemaker depolarization phase, the cardiac equivalent of the interburst interval.

In addition to the steady-state component of I_p that mostly influences the interburst interval, additional pump current activates specifically during the burst because of spike-mediated enhanced Na^+ influx. This dynamic component of I_p constrains intraburst spike frequency and generates a transient postburst AHP (Fig. 6). We propose that the dynamic component of I_p is responsible for burst termination in trigeminal motoneurons under apamin and low- Ca^{2+}/Ba^{2+} conditions. Consequently, during the ouabain-induced transitional bursting phase, the intraburst $f-t$ relationship became erratic (and ultimately broke down), and the postburst AHP consistently declined in amplitude (Figs. 3 and 4). Once I_p was fully blocked by the cardiac glycosides, every trigeminal motoneuron tested locked into the

tonic spiking state that represents a nonterminating active phase.

A similar dynamic component of I_p was characterized by Johnson et al. (1992) in rat midbrain dopaminergic neurons. Similar to our data, eliminating I_p caused cessation of NMDA-induced bursting in midbrain dopaminergic neurons. These neurons, like trigeminal motoneurons, entered a nonterminating active phase of tonic spiking. Also similar to trigeminal motoneurons, the dynamic component of I_p (the component of I_p activated specifically during bursts) in dopaminergic neurons was sufficient to terminate bursts when I_{K-Ca} was blocked pharmacologically (Johnson and Seutin 1997; Seutin et al. 1993). I_p is also crucial for burst termination in several other neuron types (Angstadt and Friesen 1991; de Waele et al. 1993; Tsai and Chen 1995). In these cells, too, blocking I_p induced tonic spiking.

Although burst termination does not critically depend on the slow inactivation of the persistent Na^+ and L-type Ca^{2+} currents, these processes probably still occur and influence burst characteristics. We showed earlier that bath application of Bay K 8644 prolongs burst duration during serotonin-induced bursting (Hsiao et al. 1998), most likely by slowing the kinetics of the L-type Ca^{2+} channels. This suggests that L-channel inactivation normally influences burst duration. Persistent Na^+ currents can also inactivate (Fleidervish et al. 1996), which could modify burst duration. Also during simulated bursts in this study (Fig. 6) the intraburst $f-t$ relationship still declined monotonically in the presence of apamin + ouabain. This suggests some temporal inactivation of the inward currents or recruitment of an unidentified outward current other than I_{K-Ca} and I_p during the simulated burst.

We propose that inactivation of the inward currents indirectly causes shorter burst duration during blockade of I_p . If the inward currents (L-type Ca^{2+} or persistent Na^+ current) inactivate to some extent during bursts they normally de-inactivate during the relatively hyperpolarized interburst interval. Because removal of the tonic component of I_p significantly shortens the interburst interval (described previously), the inward currents may not fully recover from inactivation between bursts. The magnitude of inward current available to generate subsequent bursts would then be compromised. These “compromised” bursts would then require less repolarizing current and therefore less time to terminate.

This proposal posits that less inward current underlies bursts after blockade of I_p . If this is true we would also expect an overall reduction in intraburst spike frequency after blockade of I_p , and specifically we would expect a downward shift in the intraburst $f-t$ curve. In fact, the intraburst $f-t$ curve in the presence of apamin + ouabain (Fig. 3C) was notably depressed compared with the intraburst $f-t$ curve during apamin alone (Fig. 3A). This suggests that the inward currents inactivated to some extent after application of cardiac glycosides, consequently depressing the intraburst $f-t$ curve and shortening burst duration.

In addition to blocking I_p , cardiac glycosides can induce “slip-mode conductance” in cardiac Na^+ channels, making them Ca^{2+} permeable (Santana et al. 1998). If this effect occurs in neuronal Na^+ channels it could potentially enhance inward currents during cardiac glycoside-challenged bursting and cause tonic spiking. However, we believe this effect cannot explain the current results because intraburst spike frequency

clearly decreases during the ouabain and strophanthidin experiments (e.g., Fig. 3C). Decreased intraburst spike frequency is inconsistent with enhancement of inward current.

The tonic spiking state induced by cardiac glycosides is unlikely to represent general rundown in trigeminal motoneurons caused by large shifts in the Na^+ and K^+ concentration gradients for the following reasons. In the presence of apamin + strophanthidin bursts could initiate normally (Fig. 5), and the evoked action potential was close to full amplitude (Fig. 3B, bottom).

Physiological significance

Trigeminal motoneurons exhibit bistability and bursting in the presence of serotonin (Hsiao et al. 1998), an endogenous neuromessenger associated with oral-motor behaviors (Fornal et al. 1996; Hsiao et al. 1997; Veasey et al. 1995). Although rhythmic oral-motor behaviors are produced by brain stem central pattern generators (CPGs) that project to trigeminal motoneurons (Goldberg and Chandler 1990; Lund 1976; Nakamura and Katakura 1995), the intrinsic properties of the motoneurons shape the final output pattern. In trigeminal (Hsiao et al. 1998) and spinal motoneurons (Hounsgaard et al. 1988a; Kiehn 1991; Kiehn and Eken 1997; Kiehn et al. 1996) bistability and bursting are putatively important for motor behaviors; these properties can amplify motoneuronal output in the absence of maintained synaptic excitation. Because trigeminal motoneurons possess both $I_{\text{K-Ca}}$ and I_{p} and these two currents influence the temporal characteristics of serotonin-induced bursting, neuromodulation of $I_{\text{K-Ca}}$ and I_{p} could regulate rhythmic motoneuronal spike output to match CPG activity. The regulation of I_{p} may simultaneously influence the phasic activity of the CPG because cardiac glycosides disrupt spinal networks that generate rhythmic motor patterns (Ballerini et al. 1997). In this way the intrinsic properties of trigeminal motoneurons would complement and assist the expression of ongoing spatiotemporal activity in the brain stem networks generating mastication or other rhythmic oral-motor behaviors, such as suckling, grooming, or lapping.

We thank Dr. Jens C. Rekling for a critical reading of the manuscript and M. Z. Castillo for technical contributions.

This work was funded by National Institute of Dental Research Grant RO1 DE-06193.

Address for reprint requests: S. H. Chandler, Dept. of Physiological Science, 2851 Slichter Hall, Los Angeles, CA 90095-1568.

Received 22 September 1998; accepted in final form 1 December 1998.

REFERENCES

- ANGSTADT, J. D. AND FRIESEN, W. O. Synchronized oscillatory activity in leech neurons induced by calcium channel blockers. *J. Neurophysiol.* 66: 1858–1873, 1991.
- BALLERINI, L., BRACCI, E., AND NISTRI, A. Pharmacological block of the electrogenic sodium pump disrupts rhythmic bursting induced by strychnine and bicuculline in the neonatal rat spinal cord. *J. Neurophysiol.* 77: 17–23, 1997.
- BENSON, J. A. AND ADAMS, W. B. Ionic mechanisms of endogenous activity in molluscan burster neurons. In: *Neuronal and Cellular Oscillators*, edited by J. W. Jacklet, New York: Marcel Dekker, 1989, p. 87–120.
- BERTRAM, R., BUTTE, M. J., KIEMEL, T., AND SHERMAN, A. Topological and phenomenological classification of bursting oscillations. *Bull. Math. Biol.* 57: 413–439, 1995.
- CANAVIER, C. C., CLARK, J. W., AND BYRNE, J. H. Simulation of the bursting activity of neuron R15 in *Aplysia*: role of ionic currents, calcium balance, and modulatory transmitters. *J. Neurophysiol.* 66: 2107–2124, 1991.
- CHANDLER, S. H., HSIAO, C. F., INOUE, T., AND GOLDBERG, L. J. Electrophysiological properties of guinea pig trigeminal motoneurons recorded in vitro. *J. Neurophysiol.* 71: 129–145, 1994.
- CHANDLER, S. H. AND TRUEBLOOD, P. R. Pharmacological mechanisms controlling trigeminal motoneuronal excitability. In: *Brain and Oral Function: Oral Motor Function and Dysfunction*, edited by T. Morimoto, T. Matsuya, and K. Takada, Amsterdam: Elsevier, 1995, p. 99–105.
- CURTIS, J. C. AND APPENTENG, K. The electrical geometry, electrical properties and synaptic connections onto rat V motoneurons in vitro. *J. Physiol. (Lond.)* 465: 85–119, 1993.
- DEL NEGRO, C. A., HSIAO, C.-F., CHANDLER, S. H., AND GARFINKEL, A. Evidence for a novel mechanism of bursting in rodent trigeminal neurons. *Biophys. J.* 75: 174–182, 1998.
- DE WAELE, C., SERAFIN, M., KHATEB, A., YABE, T., VIDAL, P. P., AND MUHLETHALER, M. Medial vestibular nucleus in the guinea-pig: apamin-induced rhythmic burst firing—an in vitro and in vivo study. *Exp. Brain Res.* 95: 213–222, 1993.
- EL MANIRA, A., TEGNER, J., AND GRILLNER, S. Calcium-dependent potassium channels play a critical role for burst termination in the locomotor network in lamprey. *J. Neurophysiol.* 72: 1852–1861, 1994.
- FLEIDERVISH, I. A., FRIEDMAN, A., AND GUTNICK, M. J. Slow inactivation of Na^+ current and slow cumulative spike adaptation in mouse and guinea-pig neocortical neurons in slices. *J. Physiol. (Lond.)* 493: 83–97, 1996.
- FORNAL, C. A., METZLER, C. W., MARROSO, F., RIBIERO-DO-VALLE, L. E., AND JACOBS, B. L. A subgroup of dorsal raphe serotonergic neurons in the cat is strongly activated during oral-buccal movements. *Brain Res.* 716: 123–133, 1996.
- GOLDBERG, L. G. AND CHANDLER, S. H. Central mechanisms of rhythmic trigeminal activity. In: *Neurophysiology of Jaws and Teeth*, edited by A. Taylor. London: Macmillan, 1990, p. 268–293.
- GOLDBERG, L. J., CHANDLER, S. H., AND TAL, M. Relationship between jaw movements and trigeminal motoneuron membrane-potential fluctuations during cortically induced rhythmic jaw movements in the guinea pig. *J. Neurophysiol.* 48: 110–125, 1982.
- GORMAN, A. L., HERMANN, A., AND THOMAS, M. V. Intracellular calcium and the control of neuronal pacemaker activity. *Fed. Proc.* 40: 2233–2239, 1981.
- GORMAN, A. L., HERMANN, A., AND THOMAS, M. V. Ionic requirements for membrane oscillations and their dependence on the calcium concentration in a molluscan pace-maker neurone. *J. Physiol. (Lond.)* 327: 185–217, 1982.
- GURAHIAN, S. M., CHANDLER, S. H., AND GOLDBERG, L. J. Intracellular analysis of trigeminal motoneuron rhythmic activity during stimulation of pontomedullary reticular formation in anesthetized guinea pig. *J. Neurophysiol.* 62: 1225–1236, 1989.
- HEYER, C. B. AND LUX, H. D. Properties of a facilitating calcium current in pace-maker neurones of the snail, *Helix pomatia*. *J. Physiol. (Lond.)* 262: 319–348, 1976.
- HOUNSGAARD, J., HULTBORN, H., JESPERSEN, B., AND KIEHN, O. Bistability of alpha-motoneurons in the decerebrate cat and in the acute spinal cat after intravenous 5-hydroxytryptophan. *J. Physiol. (Lond.)* 405: 345–367, 1988a.
- HOUNSGAARD, J., KIEHN, O., AND MINTZ, I. Response properties of motoneurons in a slice preparation of the turtle spinal cord. *J. Physiol. (Lond.)* 398: 575–589, 1988b.
- HSIAO, C. F., TRUEBLOOD, P. R., LEVINE, M. S., AND CHANDLER, S. H. Multiple effects of serotonin on membrane properties of trigeminal motoneurons in vitro. *J. Neurophysiol.* 77: 2910–2924, 1997.
- HSIAO, C.-F., DEL NEGRO, C. A., TRUEBLOOD, P. R., AND CHANDLER, S. H. The ionic basis for serotonin-induced bistable membrane properties in guinea pig trigeminal motoneurons. *J. Neurophysiol.* 79: 2847–2856, 1998.
- HU, B. AND BOURQUE, C. W. NMDA receptor-mediated rhythmic bursting activity in rat supraoptic nucleus neurons in vitro. *J. Physiol. (Lond.)* 458: 667–687, 1992.
- JOHNSON, S. W. AND SEUTIN, V. Bicuculline methiodide potentiates NMDA-dependent burst firing in rat dopamine neurons by blocking apamin-sensitive Ca^{2+} -activated K^+ currents. *Neurosci. Lett.* 231: 13–16, 1997.
- JOHNSON, S. W., SEUTIN, V., AND NORTH, R. A. Burst firing in dopamine neurons induced by N-methyl-D-aspartate: role of electrogenic sodium pump. *Science* 258: 665–667, 1992.
- KIEHN, O. Plateau potentials and active integration in the 'final common pathway' for motor behaviour. *Trends Neurosci.* 14: 68–73, 1991.
- KIEHN, O. AND EKEN, T. Prolonged firing in motor units: evidence of plateau potentials in human motoneurons? *J. Neurophysiol.* 78: 3061–3068, 1997.

- KIEHN, O., ERDAL, J., EKEN, T., AND BRUHN, T. Selective depletion of spinal monoamines changes the rat soleus EMG from a tonic to a more phasic pattern. *J. Physiol. (Lond.)* 492: 173–184, 1996.
- KIM, Y. I. AND CHANDLER, S. H. NMDA-induced burst discharge in guinea pig trigeminal motoneurons in vitro. *J. Neurophysiol.* 74: 334–346, 1995.
- KOBAYASHI, M., INOUE, T., MATSUO, R., MASUDA, Y., HIDAKA, O., KANG, Y., AND MORIMOTO, T. Role of calcium conductances on spike afterpotentials in rat trigeminal motoneurons. *J. Neurophysiol.* 77: 3273–3283, 1997.
- KRAMER, R. H. AND ZUCKER, R. S. Calcium-induced inactivation of calcium current causes the inter-burst hyperpolarization of *Aplysia* bursting neurons. *J. Physiol. (Lond.)* 362: 131–160, 1985.
- LÄUGER, P. Na,K-ATPase. In: *Electrogenic Ion Pumps*, edited by P. Läuger, Sunderland, MA: Sinauer, 1991, p. 168–225.
- LEGENDRE, P., MCKENZIE, J. S., DUPOUY, B., AND VINCENT, J. D. Evidence for bursting pacemaker neurons in cultured spinal cord cells. *Neuroscience* 16: 753–767, 1985.
- LI, Y.-X., BERTRAM, R., AND RINZEL, J. Modeling *N*-methyl-D-aspartate-induced bursting in dopamine neurons. *Neuroscience* 71: 397–410, 1996.
- LI, Z. AND HATTON, G. I. Oscillatory bursting of phasically firing rat supraoptic neurons in low-Ca²⁺ medium: Na⁺ influx, cytosolic Ca²⁺ and gap junctions. *J. Physiol. (Lond.)* 496: 379–394, 1996.
- LUND, J. P. Evidence for a central neural pattern generator regulating the chewing cycle. In: *Mastication*, edited by D. J. Anderson and B. Matthews, Bristol, UK: Wright, 1976, p. 204–212.
- MOSFELDT LAURSEN, A. AND REKLING, J. C. Electrophysiological properties of hypoglossal motoneurons of guinea-pigs studied in vitro. *Neuroscience* 30: 619–637, 1989.
- NAKAMURA, Y. AND KATAKURA, N. Generation of masticatory rhythm in the brainstem. *Neurosci. Res.* 23: 1–19, 1995.
- NISHIMURA, Y., SCHWINDT, P. C., AND CRILL, W. E. Electrical properties of facial motoneurons in brainstem slices from guinea pig. *Brain Res.* 502: 127–142, 1989.
- RINZEL, J. AND ERMENTROUT, G. B. Analysis of neural excitability and oscillations. In: *Methods in Neuronal Modeling: From Ions to Networks* (2nd ed.), edited by C. Koch and I. Segev. Cambridge: MIT Press, 1998, p. 251–292.
- ROSE, C. R. AND RANSOM, B. R. Regulation of intracellular sodium in cultured rat hippocampal neurons. *J. Physiol. (Lond.)* 499: 573–587, 1997.
- SAKAI, R., HAGIWARA, N., MATSUDA, N., KASSANUKI, H., AND HOSODA, S. Sodium-potassium pump current in rabbit sino-atrial node cells. *J. Physiol. (Lond.)* 490: 51–62, 1996.
- SANTANA, L. F., GOMEZ, A. M., AND LEDERER, W. J. Ca²⁺ flux through promiscuous cardiac Na⁺ channels: slip mode conductance. *Science* 279: 1027–1033, 1998.
- SEUTIN, V., JOHNSON, S. W., AND NORTH, R. A. Apamin increases NMDA-induced burst-firing of rat mesencephalic dopamine neurons. *Brain Res.* 630: 341–344, 1993.
- TAKAHASHI, T. Membrane currents in visually identified motoneurons of neonatal rat spinal cord. *J. Physiol. (Lond.)* 423: 27–46, 1990.
- TELL, F. AND JEAN, A. Ionic basis for endogenous rhythmic patterns induced by activation of *N*-methyl-D-aspartate receptors in neurons of the rat nucleus tractus solitarii. *J. Neurophysiol.* 70: 2379–2390, 1993.
- TSAI, M. C. AND CHEN, Y. H. Bursting firing of action potentials in central snail neurons elicited by D-amphetamine: role of the electrogenic sodium pump. *Comp. Biochem. Physiol. C Pharmacol. Toxicol. Endocrinol.* 111: 131–141, 1995.
- VEASEY, S. C., FORNAL, C. A., METZLER, C. W., AND JACOBS, B. L. Response of serotonergic caudal raphe neurons in relation to specific motor activities in freely moving cats. *J. Neurosci.* 15: 5346–5359, 1995.
- VIANA, F., BAYLISS, D. A., AND BERGER, A. J. Multiple potassium conductances and their role in action potential repolarization and repetitive firing behavior of neonatal rat hypoglossal motoneurons. *J. Neurophysiol.* 69: 2150–2163, 1993.
- WALLEN, P. AND GRILLNER, S. *N*-Methyl-D-aspartate receptor-induced, inherent oscillatory activity in neurons active during fictive locomotion in the lamprey. *J. Neurosci.* 7: 2745–2755, 1987.
- ZHANG, L. AND KRNEVIC, K. Apamin depresses selectively the after-hyperpolarization of cat spinal motoneurons. *Neurosci. Lett.* 74: 58–62, 1987.